Fermi Surface of Bi(111) Measured by Photoemission Spectroscopy

Christian R. Ast and Hartmut Höchst*

Synchrotron Radiation Center, University of Wisconsin–Madison, Stoughton, Wisconsin 53589

(Received 24 May 2001; published 9 October 2001)

Synchrotron radiation angle-resolved photoemission spectroscopy of Bi(111) shows that the Fermi surface consists of six elongated hole pockets along the $\overline{\Gamma M}$ directions surrounding a ring-shaped electron pocket centered at $\overline{\Gamma}$, all of which have two-dimensional character. The associated hole and electron sheet densities are $p_s = 1.1 \times 10^{13}$ cm^{-2} and $n_s = 5.5 \times 10^{12}$ cm^{-2}, respectively. A weak emission feature associated with the bulk hole pocket in the Fermi surface was identified. The Fermi momentum of the bulk hole band near the T point is $k_F = 0.013 \pm 0.003$ Å^{-1}.

DOI: 10.1103/PhysRevLett.87.177602 PACS numbers: 79.60.Bm, 71.18.+y, 73.20.–r

Bismuth, a group-V semimetal, has unique electronic properties. Its Fermi energy is only about 25 meV, the effective masses are highly anisotropic and can be up to 3 orders of magnitude smaller than the free electron mass. As a result of these properties the electronic de Broglie wavelength is about 40 nm, which is more than a factor of 100 larger than in regular metals. These characteristics make Bi a prime candidate to study the quantum size effect (QSE) in solids [1–8]. It was argued that the overlap between electron and hole bands is gradually removed while decreasing the film thickness [9]. At a critical thickness of $d \approx 23$–32 nm a band gap is predicted to develop for Bi. Even after 30 years of active research the experimental verification of a thickness dependent semimetal-semiconductor (SMSC) transition, a key element in the theoretical considerations, remains a controversial issue [10]. It is further argued that the lack of drastic changes in the low-temperature conductivity may be associated with majority-hole carriers originating from surface states and band bending effects. Experiments showed that the effective carrier concentration scales inversely proportional with film thickness. In the thin film limit magnetotransport measurements by Hoffman *et al.* [2] indicate surface charge carrier densities of $p_s \approx 8 \times 10^{12}$ cm^{-2}. Considering an intrinsic bulk charge carrier concentration of 2.5×10^{17} cm^{-3}, it is apparent that surface or interface related contributions dominate the transport properties for films $d < 30$ nm layer thickness.

From the existing experiments it is not obvious if these additional charges are a result of impurities and poor film quality or if they are associated with surface states originating from highly ordered and abruptly terminated epitaxial films and are as such unavoidable in measurements where the Bi-surface is vacuum terminated.

To further expand on these questions we have studied the electronic bulk and surface band structure of a highly ordered Bi(111) single crystal. This Letter reports Fermi surface (FS) measurements obtained by angle resolved photoemission spectroscopy (ARPES). These measurements provide strong evidence that the additional hole-majority carrier density, which is in violation of the bulk charge neutrality condition, is indeed associated with surface bands. In addition we present first measurements of the bulk Fermi surface near the T point where the hole pocket is located.

Bi crystallizes in a rhombohedral ($A7$) structure (two atoms in a basis) which can be constructed from two interpenetrating face centered cubic (fcc) lattices that are stretched and displaced along the (111) axis. The accompanied change in symmetry is in large part responsible for the semimetallic character of Bi. The reduced symmetry also changes the two L points along the trigonal axis in the Brillouin zone (BZ) into T points, resulting in six L points and two T points [11].

So far most of the Fermi surface properties of Bi were indirectly deduced from magnetotransport measurements. From Shubnikov–de Haas oscillations in the magnetoresistance and de Haas–van Alphen oscillations in the susceptibility a parabolic ellipsoidal model of the Fermi surface evolved consisting of a hole pocket along the trigonal axis and three electron pockets in the plane that contains the bisectrix and the binary axes [12–14]. As a result of the typically low intrinsic carrier concentrations in semimetals, the Fermi surface of Bi occupies only about 0.1% of the Brillouin zone volume. From these experiments a Fermi surface model evolved that was capable of describing most of the experimental findings.

Band structure calculations identify the location of the valence band maximum at the T point and the conduction band minima at the L points [15–19]. Assuming parabolic energy bands for electron and hole carriers, it was suggested that the Fermi surface consists of a rather prolate ellipsoid of hole states from band 5 (almost completely occupied p-like band) centered at the T point and oriented with the long axis parallel to the trigonal axis and three prolonged ellipsoids of electron pockets from band 6 (almost completely unoccupied p-like band). The electron ellipsoids are slightly tilted from the trigonal plane and centered at the L points.

Photoemission studies are in agreement with the basic features of the bulk band structure calculations but do not report some of the rather miniscule effects stemming from a small k-space region centered on the trigonal axis [20–24]. A more recent study by Hengsberger *et al.* [25]

provides first indications that the electronic structure close to the Fermi level is dramatically different from the well-established band structure. We performed experiments to determine the FS in the highly localized region near the T point of Bi(111). The momentum resolution was experimentally verified to be $\Delta k \leq 0.023$ Å^{-1}. The spectrometer parameters were set such that the energy resolution (determined from Au Fermi level measurements) was 25 meV for band structure maps and 40 meV for Fermi surface maps (FSM). Clean sample surfaces were obtained by cleaving samples of single crystal Bi *in situ*. The sample orientation was done using standard Laue techniques and confirmed by FSM's of the extended zone scheme displaying multiple $\overline{\Gamma}$ points. The base pressure was $\approx 10^{-8}$ Pa. Sample cleanliness was monitored indirectly through surface features whose emission intensities did not change noticably over the course of a day. In order to minimize phonon-related broadening to the photoemission spectra the sample was cooled to 50 K which is significantly below the Debye temperature of Bi ($\Theta_D = 120$ K). Contours of the FS as a function of the parallel electron momentum components can be obtained by measuring the photoemission intensity at the Fermi level and scanning the electron analyzer along the polar and azimuthal directions relative to the sample normal. The FSM shown in Fig. 1 was measured with $h\nu = 18$ eV photon energy. The image displays raw data normalized to the beam current of the storage ring. The image is not symmetrized or averaged, but was acquired by scanning the electron analyzer over the entire momentum range as indicated in the figure.

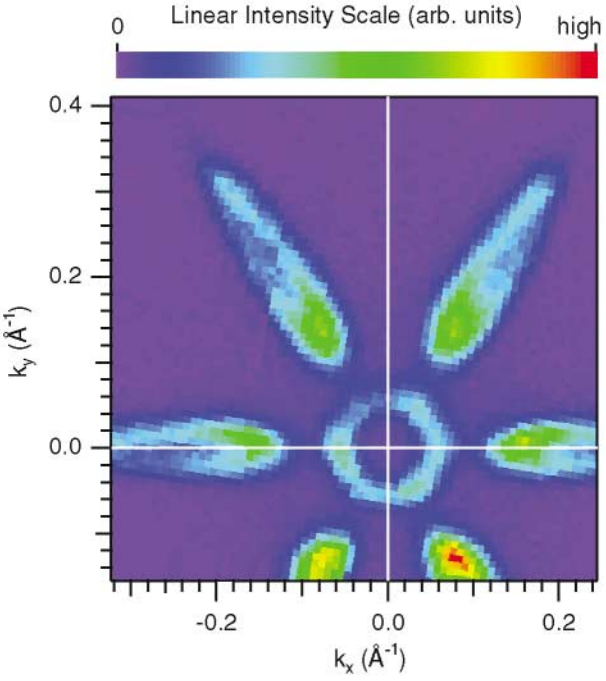

FIG. 1 (color). Intensity map at the Fermi level of Bi(111) measured at $h\nu = 18$ eV. The angular steps were 0.25°. k_x and k_y are the parallel components of the electron momentum along the $\overline{\Gamma M}$ and the $\overline{\Gamma K}$ direction, respectively.

The FSM displays a narrow ring centered on the crystal normal (trigonal axis) surrounded radially by lobes, which are 60° apart from each other. As will be shown later, the features displayed in this FSM are of a two-dimensional nature. The center ring encloses electron states, whereas the six lobes enclose hole states. To visualize the size and orientation of the Fermi surface we have superimposed an outline of the FSM from Fig. 1 onto the BZ, as shown in Fig. 2. One clearly sees that the Fermi surface contours enclose only a very small fraction of the Brillouin zone.

For rhombohedral systems bulk features are expected to show a threefold symmetry around the trigonal axis; however, the rotational symmetry of the ovals around the trigonal axis is sixfold indicating two-dimensional nature. This sixfold pattern is oriented in k space such that the ovals point to the center of the hexagonal face of the surface Brillouin zone (SBZ), i.e., they are located along $\overline{\Gamma M}$. From the energy dispersion of the band associated with the lobes it will become clear that they indeed cross the Fermi surface (see Fig. 4 below).

From the intensity map in Fig. 1 it is not possible to identify whether these features are associated with hole-like or electronlike bands. To further clarify the character of the FS pockets we used angular resolved energy distribution curves (EDC's) to determine the band dispersion $E(k_\parallel)$ along a lobe direction. Figure 3 shows the EDC's measured from $-3.25°$ to 12.75° in 0.5° steps along $\overline{\Gamma M}$. The indicated peak positions were determined by fitting independent Lorentzians and an inelastic background multiplied by the Fermi distribution function to the EDC's.

From the momentum dependence of fitted peak positions we obtain the band structure $E(k)$ along the $\overline{\Gamma M}$ direction.

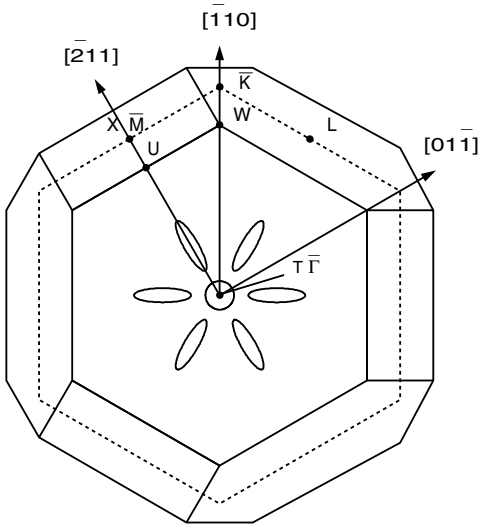

FIG. 2. Projection of the bulk Brillouin zone (solid lines) onto the (111)-surface Brillouin zone (dashed lines). The trigonal axis is perpendicular to the paper plane.

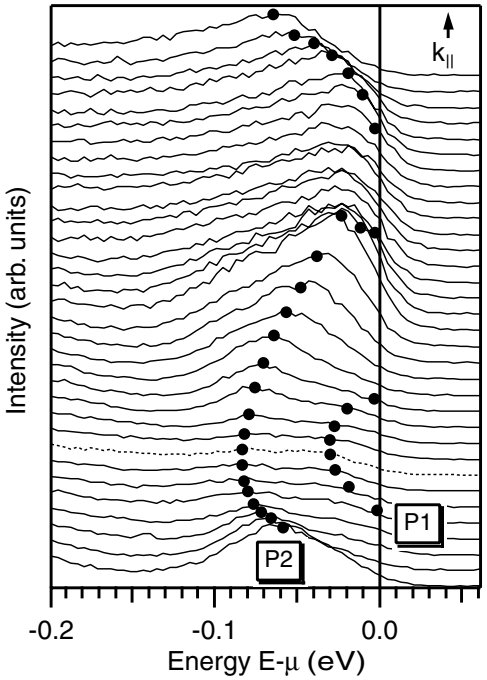

FIG. 3. EDCs of Bi(111) measured at $h\nu = 18$ eV. Dotted line: $k_{\|} = 0$ Å^{-1}. k spacing between EDC's at chemical potential μ: 0.016 Å^{-1}. The energy axis is relative to μ.

Figure 4 shows the fitted band dispersion of peaks $P1$ and $P2$ (solid lines) superimposed with the intensity image of the experimental band structure map.

$P1$ is a rapidly dispersing band with an energy minimum at $E_0 = -32.0 \pm 3.0$ meV. The dispersion is nearly parabolic with an effective electron mass of $m_e^* = 0.22 \pm 0.04$. The band associated with peak $P2$ is also centered at $\overline{\Gamma}$ with a minimum energy of $E_0 = -83.4 \pm 1.0$ meV. The band starts out at $k_{\|} = 0$ to disperse parabolically but is fitted to a higher order polynomial as it crosses the Fermi level at $k_{\|} = 0.197$ Å^{-1}. Extrapolating the polynomial fit above the Fermi level, the band reaches a maximum at $k_{\|} = 0.255$ Å^{-1} with an energy of $E_0 = 11.9$ meV and reenters the Fermi level at $k_{\|} = 0.312$ Å^{-1}. The effective hole masses at the Fermi level crossings are $m_h^* = 0.45 \pm 0.01$ and $m_h^* = 0.70 \pm 0.02$, respectively.

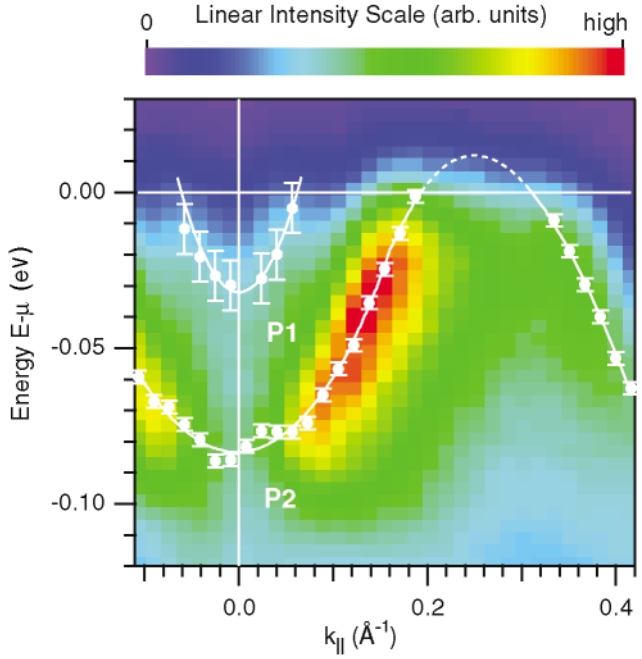

FIG. 4 (color). Band structure of Bi(111) at $h\nu = 18$ eV. $k_{\|}$ along $\overline{\Gamma M}$. Solid lines: Polynomial fit to peak positions. Energies relative to chemical potential μ.

The dispersion of bands $P1$ and $P2$ is two dimensional in nature. Varying the photon energy from $h\nu = 8$–32 eV, we found that bands $P1$ and $P2$ do not vary with $k_{\perp}$, while other emission features located deeper in the valence band structure, however, do show three-dimensional dispersion.

Having identified the hole pockets at the Fermi level as truly two-dimensional features, it is straightforward to estimate the hole-carrier density. From the absolute k-space area occupied by the six lobes we find the hole-sheet density at the (111) surface of Bi to be $p_s = 1.1 \times 10^{13}$ cm^{-2}. This unambiguous determination of the hole-carrier density compares well with $p_s \approx 8 \times 10^{12}$ cm^{-2} estimated by Hoffman *et al.* from low temperature magnetotransport measurements from thin Bi films. From the inner ring, with a radius of $k_{\|} = 0.059$ Å^{-1} at the Fermi level, we extract a sheet electron density of $n_s = 5.5 \times 10^{12}$ cm^{-2} which is not too far off from $n_s = 2.75 \times 10^{12}$ cm^{-2} reported by Komnik *et al.* for their thin film approximation [6].

Knowing that the generally accepted bulk Fermi surface model of Bi consists of an elongated ellipsoid centered at the T point one might be tempted to assign the inner ring feature seen in the FSM of Fig. 1 to be the perpendicular cross section of the ellipsoid. This is not the case, because the band associated with the ring feature has truly two-dimensional character and is an electronlike band rather than a holelike band as expected from the bulk band structure. The radius of the ring, the Fermi momentum k_F, is constant and independent of $k_{\perp}$. However, by changing the excitation energy, we do see additional structures evolve inside the ring. These features can be seen most pronounced in a momentum distribution curve (MDC) rather than the more commonly used set of EDC spectra. The photon energy dependence of the emission features around the Fermi level is shown in Fig. 5 for selected photon energies.

The spectrum in Fig. 5a shows two peaks which can be attributed to the band $P1$ in Fig. 4. The position of the two peaks is independent of photon energy as expected from 2D features; however, as shown in Fig. 5b two additional features (BS) emerge between the two peaks (SS) reaching maximum separation at $h\nu = 9.5$ eV. The two inner peaks (BS) are bulk features, because they appear and disappear as a function of photon energy, indicating three-dimensional behavior. They can be attributed to the valence band forming the bulk hole pocket at the T point.

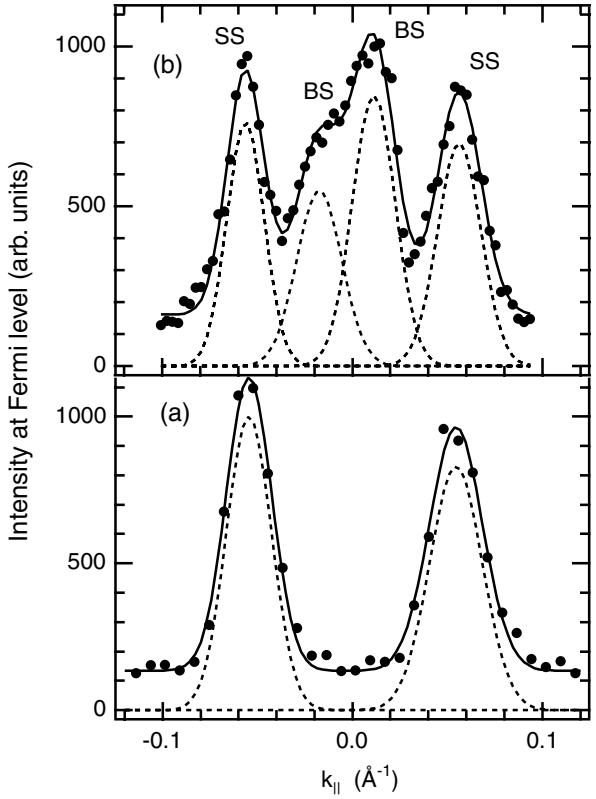

FIG. 5. MDCs of Bi(111) measured at the Fermi level at (a) $h\nu = 17$ eV and (b) $h\nu = 9.5$ eV along $\overline{\Gamma K}$. The outer peaks can be attributed to a two-dimensional state and the inner two peaks show the band forming the hole pocket.

The MDC data can be simulated by a free fit with four Gaussians. The two outermost peaks (SS) have a full width at half maximum momentum broadening of $\Gamma_{SS} = 0.024 \pm 0.003$ Å^{-1}. The bulk states (BS) are slightly broader with a width of $\Gamma_{BS} = 0.028 \pm 0.003$ Å^{-1}. We have found that the momentum broadening and the relative intensities of the SS and BS features critically depend on the cleavage quality of the crystal surface. The intensity asymmetries of the SS and BS structures are due to slight misalignment of the crystal axis with respect to the analyzer plane. From the fitted positions of inner peaks (BS) we obtain the bulk Fermi momentum $k_F = 0.013 \pm 0.003$ Å^{-1}. This value compares well with values obtained from de Haas–van Alphen measurements and band structure calculations ranging from $k_F = 0.01$–0.014 Å^{-1} [17,19].

In summary, we have measured the Fermi surface of Bi(111) single crystals by angle resolved photoemission spectroscopy. The Fermi surface map is dominated by two-dimensional hole and electron pockets. In addition we identified a rather localized emission feature of the bulk Fermi surface. The cross section of that feature is in the plane containing the T point (hole pocket). The bulk Fermi momentum in this plane is $k_F = 0.013 \pm 0.003$ Å^{-1}. The surface charge carrier densities of the holes and electrons are 1.1×10^{13} and 5.5×10^{12} cm^{-2}, respectively. Our results show that the majority carrier concentration originating from the surface can be a major contribution affecting the quantum size effect measurements in Bismuth nanostructures.

The authors would like to express their gratitude to L. A. Morales and J. J. Joyce for providing us with Bi single crystals. The Synchrotron Radiation Center (SRC) is funded by the National Science Foundation (NSF) under Award No. DMR-0084402.

*Corresponding author.
Email address: hhochst@facstaff.wisc.edu

[1] H. T. Chu, Phys. Rev. B **51**, 5532 (1995).
[2] C. A. Hoffman *et al.,* Phys. Rev. B **48**, 11 431 (1993).
[3] J. A. van Hulst *et al.,* Phys. Rev. B **52**, 5953 (1995).
[4] M. Lu *et al.,* Phys. Rev. B **53**, 1609 (1996).
[5] Y. F. Ogrin *et al.,* Sov. Phys. JETP **26**, 714 (1968).
[6] F. K. Komnik and V. V. Andrievskii, Sov. J. Low Temp. Phys. **1**, 51 (1975).
[7] N. Garcia, Y. H. Kao, and M. Strongin, Phys. Rev. B **5**, 2029 (1972).
[8] S. Takaoka and K. Murase, J. Phys. Soc. Jpn. **54**, 2250 (1985).
[9] V. B. Sandomirskii, Sov. Phys. JETP **25**, 101 (1967).
[10] D. D. Franket and H. T. Chu, Phys. Rev. B **61**, 13 183 (2000).
[11] M. H. Cohen, L. M. Falicov, and S. Golin, IBM J. Res. Dev. **8**, 215 (1964).
[12] R. D. Brown, R. L. Hartmann, and S. H. Koenig, Phys. Rev. **173**, 598 (1968).
[13] A. L. Jain and S. H. Koenig, Phys. Rev. **127**, 442 (1962).
[14] V. S. Edel'man, Adv. Phys. **25**, 555 (1976).
[15] M. H. Cohen, Phys. Rev. **121**, 387 (1961).
[16] S. Golin, Phys. Rev. **166**, 643 (1968).
[17] X. Gonze, J. P. Michenaud, and J. P. Vigneron, Phys. Rev. B **41**, 11 827 (1990).
[18] J. H. Xu, E. G. Wang, C. S. Ting, and W. P. Su, Phys. Rev. B **48**, 17 271 (1993).
[19] Y. Liu and R. E. Allen, Phys. Rev. B **52**, 1566 (1995).
[20] F. Patthey, W.-D. Schneider, and H. Micklitz, Phys. Rev. B **49**, 11 293 (1994).
[21] G. Jezequel, J. Thomas, and I. Pollini, Phys. Rev. B **56**, 6620 (1997).
[22] A. Tanaka *et al.,* Surf. Sci. **433–435**, 647 (1999).
[23] A. Tanaka *et al.,* Phys. Rev. B **59**, 1786 (1999).
[24] J. Thomas, G. Jezequel, and I. Pollini, J. Phys. Condens. Matter **11**, 9571 (1999).
[25] M. Hengsberger *et al.,* Eur. Phys. J. B **17**, 603 (2000).